

Article

Degradation Characteristics of Environment-Friendly Bamboo Fiber Lunch Box Buried in the Soil

Huan Jiang^{1,2}, Ge Wang^{1,*}, Fuming Chen^{2,*} , Xiaoyi Chen^{1,2} and Xin Wei^{1,2}

¹ International Centre for Bamboo and Rattan, Beijing 100102, China; jianghuan478@gmail.com (H.J.); chenxy@icbr.ac.cn (X.C.); weixin199522@gmail.com (X.W.)

² National Forestry and Grassland Administration/Beijing Co-Build Key Laboratory of Bamboo and Rattan Science Technology, Beijing 100102, China

* Correspondence: wangge@icbr.ac.cn (G.W.); fuming@icbr.ac.cn (F.C.)

Abstract: The research on the development of lunch boxes made of clean, environment-friendly, and naturally degradable plant fibers has attracted enormous attention. A bamboo fiber lunch box prepared by the clean and efficient steam explosion method has the advantages of good stiffness, water and oil resistance, and easy degradation. The purpose of this study was to investigate the degradation behavior of the environment-friendly bamboo fiber lunch box under indoor soil burial, as represented by the changes in physical properties, mechanical strength, chemical components, morphological structure, and so on. The results showed that: with the extension of the burial time, the weight loss increased rapidly from slowly to quickly; the boxes were completely degraded in the soil on the 70th day; the microorganisms in the soil first decomposed the tapioca starch, hemicellulose, and cellulose in the lunch box, and finally decomposed the lignin; the residual debris in the soil was further decomposed into CO₂, H₂O, and inorganic salts. In short, the degradation process of the lunch box mainly included the following stages: stage I: the increase in apparent roughness, the generation of microcracks, the rapid increase in weight loss, and the breakdown of starch and hemicellulose; stage II: the slow increase in the weight loss rate of the box fragmentation, the rapid decay of the mechanical strength, and the cellulose decomposition; stage III: the decomposition of lignin, the complete degradation of the debris, and the integration with the soil.

Keywords: bamboo fiber; degradation; environment-friendly lunch box; soil



Citation: Jiang, H.; Wang, G.; Chen, F.; Chen, X.; Wei, X. Degradation Characteristics of Environment-Friendly Bamboo Fiber Lunch Box Buried in the Soil. *Forests* **2022**, *13*, 1008. <https://doi.org/10.3390/f13071008>

Academic Editor: Antonios Papadopoulos

Received: 28 May 2022

Accepted: 24 June 2022

Published: 27 June 2022

Publisher's Note: MDPI stays neutral with regard to jurisdictional claims in published maps and institutional affiliations.



Copyright: © 2022 by the authors. Licensee MDPI, Basel, Switzerland. This article is an open access article distributed under the terms and conditions of the Creative Commons Attribution (CC BY) license (<https://creativecommons.org/licenses/by/4.0/>).

1. Introduction

The annual sales and the growth rate of disposable lunch boxes continued to increase in the 20th century due to their advantages of convenience and low price. They are widely used in the fields of groceries, packaging and distribution, and high-speed train meals. In 2019, the consumption of disposable plastic lunch boxes in China exceeded 40 billion [1], and considering the surge in the number of takeaway orders under the global COVID-19 epidemic, the demand for disposable lunch boxes may increase significantly in the future [2]. The plastic lunch box is light and inexpensive, but it is not easy to decompose and its natural degradation may take hundreds of years [3]. When these lunch boxes are discarded and exposed to the natural environment, they gradually decompose into pieces of smaller sizes, such as microplastics (0.1 μm to 5 mm) and nanoplastics (<0.1 μm), which are continuously transferred from land to rivers, lakes, and oceans, and eventually enter the food chain, threatening the biological health and the ecological environment [4–8]. Since the gradual emergence of the problem of disposable plastic lunch boxes, many countries and regions have successively promulgated “plastic restriction” and “plastic ban” policies. Developing and using environmental-friendly and degradable lunch boxes are important to replace the disposable plastic boxes and to improve the ecological, environmental protection, and economic values [9].

At present, the most common lunch boxes are lunch boxes made of biodegradable plastic, paper pulp, plant fiber, starch, and so forth. Among these, the mainstream are boxes constructed of plant fibers and synthetic polyesters, such as polylactic acid (PLA) and polycaprolactone (PCL) [10–12]. The plant fiber lunch box is an environment-friendly lunch box with a certain strength and easy degradation. It is made of natural plant fibers such as bamboo fiber, bagasse, rice husk, straw, hemp fiber, and coconut shell. However, most natural plant fibers have strong hygroscopicity and poor mechanical properties [13]. While making lunch boxes, they are usually supplemented with water and oil repellents, plastic coatings, sizing, and modification methods [14–16] to improve their performance, in terms of anti-penetration, temperature resistance, stiffness, and appearance quality. However, adding industrial additives, coatings of waxy layers, and toxic substances such as plasticizers, heavy metals, paraffin, fluorescent agents, and calcium carbonate are not conducive to rapid degradation after disposal. The migration of degradation products also has adverse effects on the human body and the soil environment [17]. Synthetic polyester lunch boxes include degradable lunch boxes made of PLA, PHA (polyhydroxyalkanoates), PBAT (poly butylene adipate-co-terephthalate), and so forth. For example, PLA lunch boxes are made of biomass raw materials such as corn, sugarcane, sugar beet, and other fermentation products. They have high strength and good stability. However, the molecular structure of the polyester materials is stable, and the degradation cycle in the soil is long. Some studies have shown that the degradation takes at least 4 months or even longer [18,19].

Many studies were conducted on the soil burial degradation of degradable plant-based utensils. Ferreira et al. [20] investigated biodegradable trays made of cassava starch mixed with sugarcane bagasse and supplemented with different mass fractions of cornhusk, malt bagasse, or orange bagasse, and concluded that trays containing more than 20% orange bagasse were completely degraded in terms of weight loss rate within 60 days. Buxoo et al. [21] used pineapple peel, orange peel, and Mauritius hemp as raw materials to produce biodegradable disposable paper cups, and found that the 40:60 hemp-pineapple peel composite cup was completely biodegraded in the soil and sand environments within 5 and 6 weeks, respectively, in terms of weight loss rate. Although the plant-based utensils are easy to degrade, the mechanical properties are not as good as the polyester utensils, where the latter has a longer degradation time. Bamboo has excellent flexibility and toughness properties at the macro level and bamboo fiber has high strength mechanical properties, a slimming ratio, and a lower microfibril angle (MFA = 10°) [22,23]. The bamboo fiber lunch box is mechanically strong during service, demonstrating a unique balance between durability and degradability, which neither polyester lunch boxes nor pulp lunch boxes can provide. Some studies used plant fibers laminated with biodegradable polyesters to explore their degradation properties in the soil, including mechanical resistance, micromorphology, and weight loss, and degradation mechanism affected by environmental factors and the structural characteristics of fibers [24–27]. To sum up, no studies have been performed on bamboo fiber lunch boxes with degradability expressed in terms of weight loss, physical properties, chemical composition, and so on.

In this study, the environment-friendly bamboo fiber lunch box was made by mixing the bamboo fiber and a small amount of tapioca starch, with no additives added. This study provided a thorough description and complete image of the lunch boxes' degradation process, including physical and mechanical properties, chemical components, and morphological structure. In addition, the soil degradation law provided a scientific basis for the natural degradation and the secondary value-added use of lunch boxes.

2. Materials and Methods

2.1. Materials

The environment-friendly bamboo fiber lunch box was made from 2- to 3-years-old bamboo (*Bambusa pervariabilis* McClure × *Dendrocalamopsis daii* Keng f.) grown in Chongqing province, China. First, natural bamboo fibers with a diameter of 0.03–0.4 mm and a length of 10–250 mm were obtained when the raw bamboo was cut and broken, softened to obtain

loose fibers, washed and bleached, dewatered, and dried. Second, bamboo fibers were steamed and combined with a tiny amount of tapioca starch in a 97:3 mass ratio. Tapioca starch was used to fill gaps caused by the uneven distribution of bamboo fibers during the molding process, as well as to increase the lunch box's leak-proofing and strength. Third, the method of coarse and fine grinding was used to form a pulp with a beating degree of $37 \pm 2^\circ$ SR. Finally, the pulp was vacuum-filtered and molded at a temperature of 140°C for 3 min. The weight of the lunch box was about 20 g, and the load-bearing was more than 300 N. Figure 1 shows the production process for the bamboo fiber lunch box and the nutrients provided to the bamboo forest after degradation.

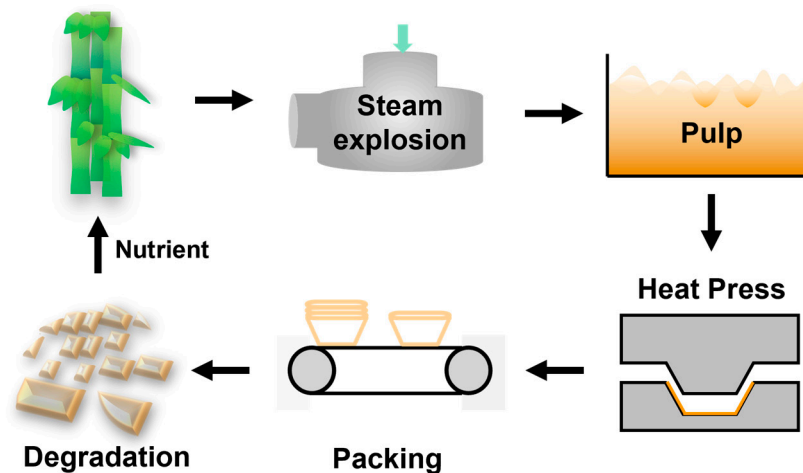


Figure 1. Preparation and degradation of an environmental-friendly bamboo fiber lunch box.

2.2. Disintegration and Biodegradability

According to the method “C soil landfill test” in the national standard GB/T 19275-2003 “Evaluation of the potential biodegradation and disintegration ability of materials under the action of specific microorganisms” [28], the degradation performance of the lunch box was determined. The square-sheet-shaped sample ($3 \times 3\text{ cm}^2$) and the dumbbell-shaped sample (refer to the 5-type sample in GB/T 1040.3-2006 [29]) were buried in loose soil 5 cm below the surface layer. The soil was collected from the pastoral soil in the Huimin area, Binzhou, Shandong province, with a relative humidity of 70–90%, pH of 7–8, and temperature of $22\text{--}25^\circ\text{C}$. The sample was taken out during the corresponding period, and the soil moisture was maintained at 70–90% by watering throughout the process, while the room temperature was maintained at $22\text{--}25^\circ\text{C}$. The soil from the specimen's surface was removed and the sample was dried in an oven at 103°C until completely dry.

Five square-sheet-shaped blank samples were taken, baked at 103°C until they were absolutely dry, and placed under 0% humidity for 1 week. The average weight was taken as M_i . The dried sample was taken out every 7 days and weighed as M_f , and the weight loss rate was calculated using Equation (1) [30].

$$\text{Weight loss (\%)} = (M_i - M_f) / M_i \times 100\% \quad (1)$$

2.3. Tensile Properties

The mechanical properties of the samples in different degradation stages were tested using a universal mechanical testing machine (MTS Systems, Co., Ltd., Beijing, China). The tensile strength of the samples was tested according to GB/T 1040.3-2006 [29]. Dumbbell-shaped specimens, 115 mm long, 25 mm wide, and 0.6 mm thick, were stretched at a rate of 2 mm/min until they fractured. Each group of samples was tested five times in parallel, and the average value was taken.

2.4. Scanning Electron Microscopy

The dried square flake samples were taken in the corresponding degradation stage, and macro-degradation images were obtained.

The microstructure and morphology were observed using a scanning electron microscope (FE-SEM, XL30, FEI, USA) to understand the changes in surface morphology. Before the test, the samples were dried and observed after coating with gold at $1000\times$ magnifications, corresponding to $10\ \mu\text{m}$.

2.5. Thermogravimetric Analysis/Derivative Thermogravimetry (TGA/DTG)

A thermogravimetric analyzer (TA Instruments, NJ, USA) was used to determine the thermal stability and degradation of the lunch box in different degradation stages. The sample, weighing approximately 5 mg, was heated in a crucible. The test atmosphere was N_2 , the heating rate was $10\ ^\circ\text{C}/\text{min}$, and the reaction temperature was $50\text{--}600\ ^\circ\text{C}$.

2.6. Fourier Transform Infrared Spectroscopy (FTIR)

The samples in different degradation stages were dried and ground with potassium bromide at a ratio of 1:100. The wavelength ranged from 4000 to $400\ \text{cm}^{-1}$, and the number of scans was 32 (VERTEX 80 V, Bruker, Germany).

2.7. Chemical Composition

Chemical composition determination was conducted using the Van Soest method [31]. The undissolved residue from boiling plant-based feeds with neutral detergent was neutral detergent fiber (NDF), comprising primarily cell wall components such as cellulose, hemicellulose, lignin, and silicate. Acid detergent was used to treat the plant-based feed, and the waste was acid detergent fiber (ADF), which contained cellulose, lignin, and silicate. The residue of ADF after 72% sulfuric acid treatment comprised lignin and silicate, and this residue was deducted from the ADF value to determine the cellulose percentage of the feed. The acid detergent lignin (ADL) content of the residue after 72% sulfuric acid treatment was determined with the fraction that escaped during ashing. The samples from each degradation date were crushed into a 60-mesh powder, dried, and prepared for use. The test was repeated twice, with the findings averaged.

$$\text{Cellulose content} = \text{ADF (\%)} - (\text{ADL} + \text{ash});$$

$$\text{Hemicellulose content} = \text{NDF (\%)} - \text{ADF (\%)};$$

$$\text{Lignin content} = \text{residue (\%)} - \text{ash (\% silicate)}.$$

2.8. X-ray Diffraction (XRD)

Determining crystallinity is an approach for understanding the effect of weathering on wooden materials [32]. The relative crystallinity of the bamboo lunch box was measured with an X-ray diffractometer (Bruker, Karlsruhe, Germany) under the following conditions: X-ray tube, copper target; voltage: 40 kV; current: 40 mA; scanning speed: $5^\circ/\text{min}$; step size: 0.02° . The sample powder (60 mesh) was pressed into thin slices at $30 \pm 2\ ^\circ\text{C}$ and then scanned from 5° to 60° in the reflection mode of the XRD. According to the peak intensities at $2\theta = 22^\circ$ and 18° , the relative crystallinity was calculated using Segal's empirical method (Equation (2)) [33]:

$$\text{CrI\%} = (I_{002} - I_{am}) / I_{002} \quad (2)$$

3. Results and Discussion

3.1. Weight Loss

Figure 2 shows the weight loss of the bamboo fiber lunch box in the soil over time. The weight loss rate increased in the first 21 days, from 10.7% on Day 7 to 25.9% on Day 21. This could be due to the loss of the bound water in the sample due to the interaction between the environment and microorganisms, as well as the fact that such easily decomposed

components with high hygroscopicity, such as tapioca starch and hemicellulose, were decomposed by microorganisms [34].

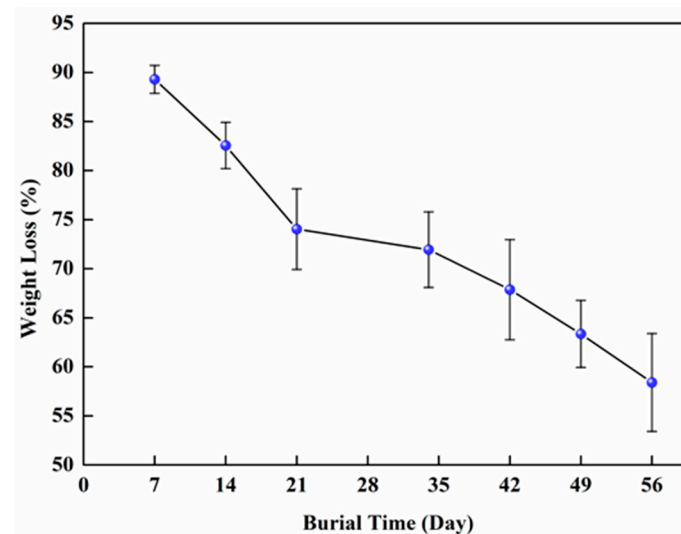


Figure 2. Weight loss of environment-friendly bamboo fiber lunch box in different degradation stages.

From Day 21 to Day 34, the weight loss rate increased and was 28.1% (Day 34). At this time, the decay of the lunch box sheets by the microorganisms showed a delay. On the one hand, the microbes tried to adapt to the environment and utilize the films as the sole carbon source to grow and multiply. This stage could be referred to as the lag phase and the logarithmic growth phase of the microbes [34]. On the other hand, the decay was relatively slow due to the tight structure of bamboo fibers.

The weight loss rate increased from Day 34 to Day 56: 32.1% (Day 42), 36.6% (Day 49), and 41.6% (Day 56) because microorganisms formed a dense and stable biofilm at this time. The loss of moisture-absorbing and decomposing substances led to the formation of a loose interwoven structure of bamboo fibers, making the fibers more prone to breakage and increasing the pore size in the sheets. The fragments of the boxes became dispersed in the soil and were assimilated by microorganisms until they vanished after 70 days. Compared with other plant-based utensils [21,35], the deterioration time was similar.

3.2. Macroscopic Images

Figure 3 shows the visual changes in the degradation of the lunch box. The initial photo of the degradation was a complete square. The surface of the sample became rough after 14 days of degradation, and the diffuse reflection increased [36,37], resulting in a deepening of the color of the flakes. In addition, the local yellowing phenomenon occurred due to the combined action of water molecule penetration during soil burial and microorganism reproduction on the sample surface [38]. The flakes became moldy and black as the degradation time (49 days) increased due to soil attachment and microorganism metabolism. The square-shaped lunch box specimens were irregular in shape on the 56th day of degradation due to the disintegration of the fiber matrix or its shedding in the soil. The lunch box had entirely decayed by the time it was buried for 70 days. On day 70, only bits and pieces of the debris from the lunch boxes were visible in the soil and could not be photographed.

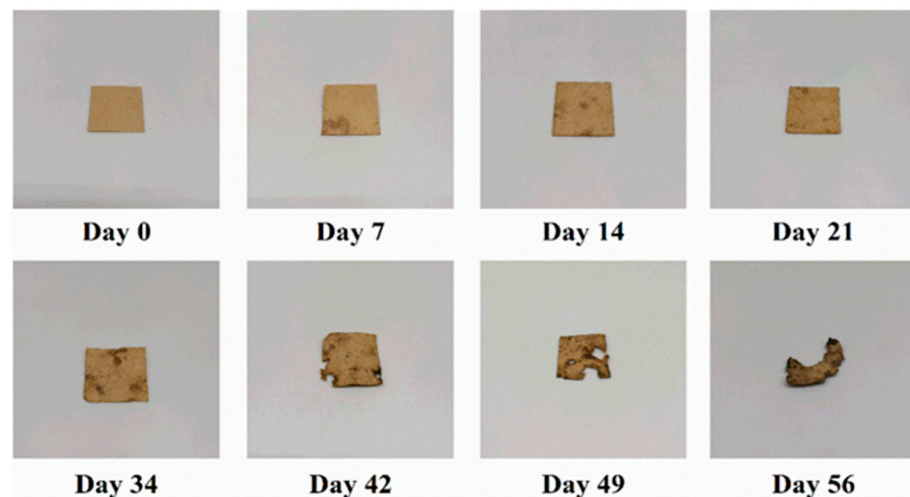


Figure 3. Macroscopic images of environment-friendly bamboo fiber lunch box in different degradation stages.

3.3. Tensile Strength

Figure 4 shows the tensile strength of the lunch box with different degradation times. As the mechanical strength of the lunch box was close to 0 after the 21st day, a relatively concentrated sampling was carried out in the early stage of degradation to observe the changes in mechanical strength. As shown in Figure 4, with the increase in burial time, the tensile strength showed a decreasing trend from slow to fast, which was as follows: 44.5, 40.8, 37.9, 24.9, 20.3, 17.9, 16.9, and 9.4 MPa. The tensile strength decreased slowly in the early stage of degradation. On the one hand, the microorganisms displayed an adaptation process in the early stage of degradation. This was consistent with the results of color darkening caused by microbial activity on the surface of the specimens [39]. On the other hand, the decomposition of the tapioca starch, hemicellulose, and connecting fibrils did not affect the strength of the entire fiber matrix. The rapid decline in mechanical properties in the later stage was attributed to a significant increase in interfiber voids, weakening of fiber adhesion, debonding of the fiber as a whole, and decay and rupture of the fibers due to the decomposition of the main chemical components [40].

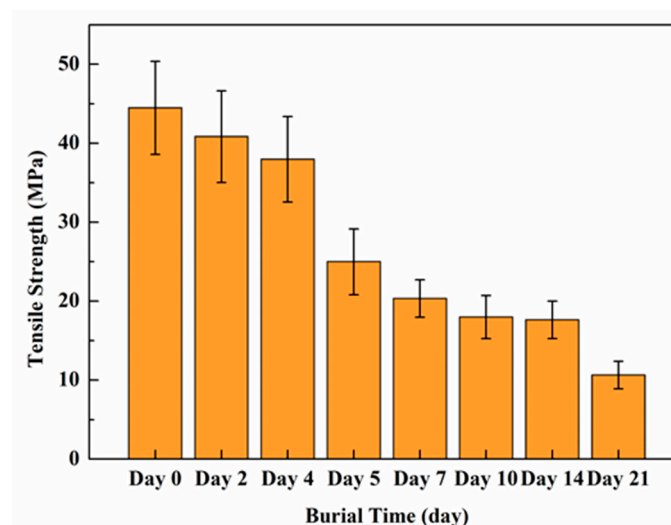


Figure 4. Tensile strength of environment-friendly bamboo fiber lunch box in different degradation stages.

3.4. Thermal Property

The thermal properties of samples after the soil burial test are presented in Figure 5. Figure 5a shows the weight loss curve for the lunch box with temperature. The process had three main stages. The first stage of the weight loss was dependent on the temperature ranging from 50 °C to 200. This stage was attributed to moisture evaporation from the sample, and the chemical composition was basically unchanged [41]. The first stage of degradation showed a loss of around 10% of the initial weight. The temperature in the second stage was 200–500 °C, which was the main weight-loss stage of pyrolysis, including the decomposition of hemicellulose, lignin, and cellulose [42]. The second stage of degradation showed a loss of more than 70% of weight. The third stage represented the end of thermal degradation and ensured that all the components of fibers were thermally degraded at temperatures beyond 600 °C, and the final remaining mass reached 20% as ash and char content [43]. Figure 5b depicts the DTG curve, which represents the variation in the weight loss rate with time, and the horizontal coordinate corresponding to its trough is the temperature point with the greatest weight loss.

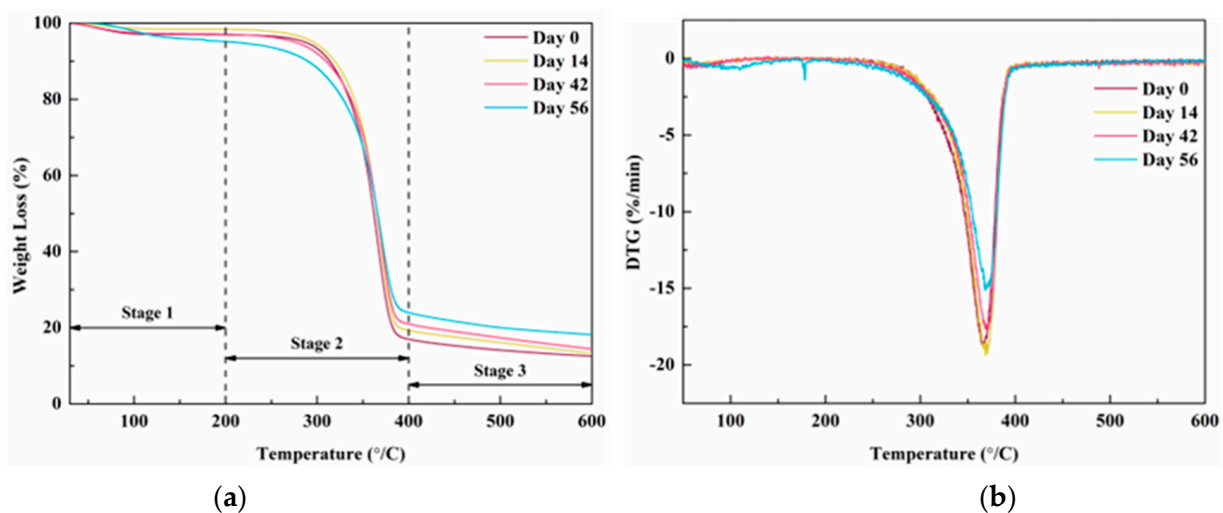


Figure 5. Thermal properties of environment-friendly bamboo fiber lunch box in different degradation stages: (a) TG; (b) DTG.

Table 1 shows the curve of the thermal decomposition rate of the lunch box with temperature in different degradation stages. The onset degradation temperature (T_o) was defined as the 1% weight loss drawn from the TG curves after 200 °C, and the residual mass at 600 °C was weight loss (%) at endset temperatures [44]. The temperature T_m at which the weight loss rate was greatest was represented by the temperature corresponding to the trough. The thermal degradability of hemicellulose and lignin was in the temperature range of 200–300 °C and 300–450 °C [45]. As shown in Table 1, with the increase in time of the soil burial test, T_o decreased from 231.5 °C to 184.9 °C, as a result of the decomposition of hemicellulose and tapioca starch that were less stable and that easily absorbed the moisture. With the prolongation of the degradation time, T_m increased continuously, from 367.3 °C to 373.8 °C. This was because hemicellulose and cellulose degraded first, the content of lignin with a higher thermal decomposition temperature increased, and the temperature increased. The residual mass at 600 °C, that is, the ash mass after the fiber has been burned, tended to increase over degradation time, which also indicated that the chemical components of the bamboo fiber died continuously during the degradation process, resulting in a higher residual mass.

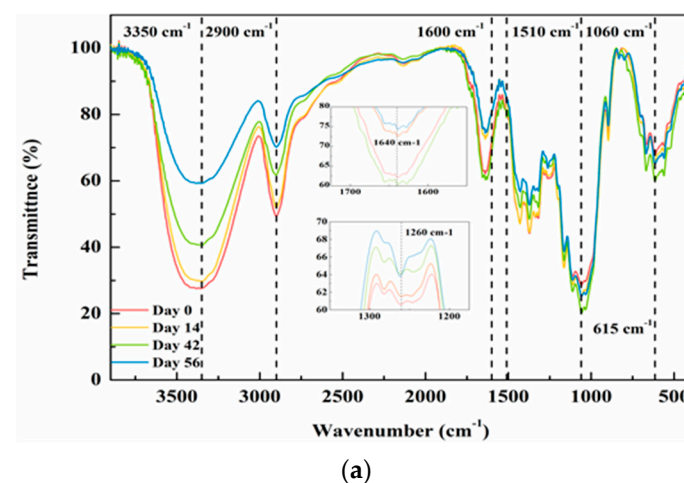
Table 1. Main thermal performance parameters of environment-friendly bamboo fiber lunch box in different degradation stages.

Burial Time (Day)	T _o (°C)	T _m (°C)	Residual Mass (%) @600 °C
0	231.5	367.3	12.5
14	220.7	368.8	13.2
42	211.8	371.7	14.4
56	184.9	373.8	18.2

3.5. Chemical Composition

Figure 6a shows the infrared spectrum of the lunch box before and after degradation. Figure 6b shows the corresponding specific content changes in cellulose, hemicellulose, and lignin. The infrared spectrum showed that the types and positions of the absorption peaks did not change significantly, but the intensities of all absorption peaks were weakened to a certain extent with the prolongation of degradation time. On the 14th day of soil burial (stage I), a slight decrease in peaks at 3350 cm^{-1} , 2900 cm^{-1} , 1060 cm^{-1} , and 615 cm^{-1} was observed, indicating that substances with hydroxyl, aliphatic, β -glycosidic, and polysaccharide regions began to degrade, respectively. The corresponding assignments of these functional groups were cellulose and hemicellulose [46]. This was consistent with the conclusion that the contents of cellulose and hemicellulose, as shown in Figure 6b, also decreased slightly, and the relative content of lignin increased. It was speculated that the initial stage of degradation (Day 14) was mainly the degradation of cellulose and hemicellulose. The initial microbial response to lignin was not strong [47].

Beginning on the 42nd day of soil burial (stage II), persistently weaker peaks were observed at 3350 cm^{-1} , 2900 cm^{-1} , and 1060 cm^{-1} in the infrared spectrum, indicating that, from the 14th day to the 42nd day, more hemicellulose was degraded. The content of hemicellulose, as shown in Figure 6b, also decreased from 10.3% to 9.1%. At this time, the relative content of lignin also decreased from 17.3% to 11.7%. The infrared spectrum showed that the peak intensity at 1600 cm^{-1} and 1510 cm^{-1} (lignin aromatic skeleton vibration) decreased [48]. The non-crystalline region of cellulose was easily decomposed, and when amorphous substances in cellulose were dissipated, the cellulose content decreased slightly from 64.2% to 63.4%.

**Figure 6.** Cont.

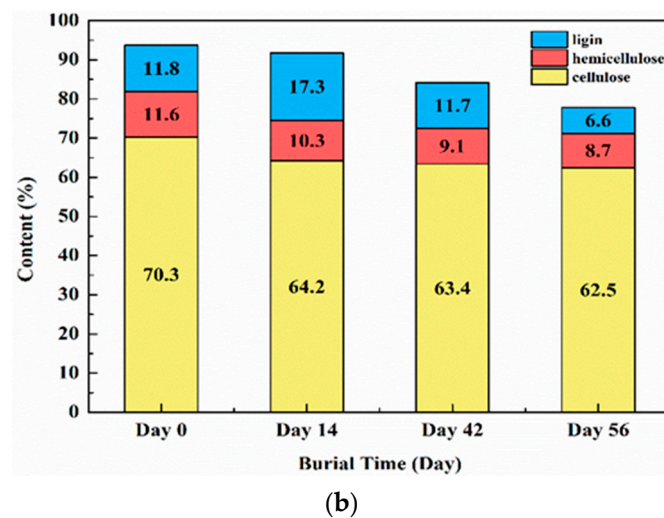


Figure 6. Infrared spectrum and three-element content images of environment-friendly bamboo fiber lunch box in different degradation stages: (a) infrared spectrogram; (b) three-element content.

On the 56th day of degradation (stage III), an increase in peaks at 1640 cm^{-1} (aromatic ring) and 1260 cm^{-1} (aryl ether or phenol) was observed in the infrared spectrum [49] mainly due to the later degradation of lignin. More aromatic structures and aromatic compounds appeared after lignin started to degrade. At the same time, most of the peak intensities in the hydroxyl, aliphatic, and polysaccharide regions continued to decrease, and the relative content of hemicellulose greatly reduced to 8.7% on the 56th day. After the rapid degradation of lignin as the main cross-linking substance and the continuous decomposition of hemicellulose, the material of the bamboo fiber lunch box gradually decomposed into small fragments.

3.6. Relative Crystallinity

In the early stages, degradation occurred easily in the amorphous regions of the lunch box, which included tapioca starch, hemicellulose, and amorphous regions of cellulose. Macroscopically, the relative crystallinity increased. Figure 7 shows that the relative crystallinity of the lunch box increased from 40.56% on Day 0 to 42.19% on Day 14. However, in the later stage, the crystalline regions interacted with the water and microorganisms. More specifically, the decomposition of the cellulose at the molecular level was achieved by either enzymatic activity (proteolysis) or fission by water molecules (hydrolysis) [40]. The cellulose molecular chain was degraded to a certain extent, the interaction between molecules decreased, and the degradation site gradually transitioned to the crystallinity area, destroying the main structure of the fibers. The crystallinity showed a downward trend; it decreased to 40.45% on the 42nd day and 34.04% on the 56th day.

3.7. Microscopic Appearance

The scanning electron microscopic images in Figure 8a reflect the changes in the surface microscopic morphology of the lunch box during different degradation periods, showing the process from the smooth surface on Day 0 to the fiber breakage on the 56th day. The following description can be seen in Figure 8a at the red arrows and circles. A large number of connecting filaments were found between the fibers of the lunch box on Day 0. The fibers closely overlapped, and the surface was dense and smooth. On the 14th day of degradation, the connecting fibrils between the fibers began to break, the overall surface of the fibers became rough, and the number of interstices between the fibers increased. On the 42nd day, some broken fibers protruded from the surface, and the roughness further increased. Cracks and pits appeared on the lamination surface formed after molding, which had a greater impact on the strength of the sample. On the 56th day, different types of

holes and grooves appeared on the fiber matrix. The fibers were dispersed as a whole, the entanglement points were greatly reduced, and fiber breakage was common.

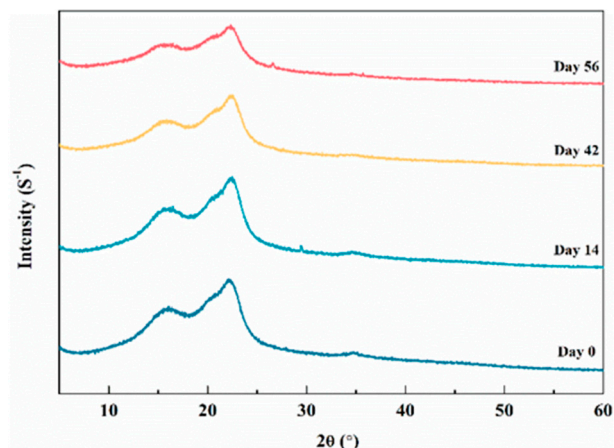
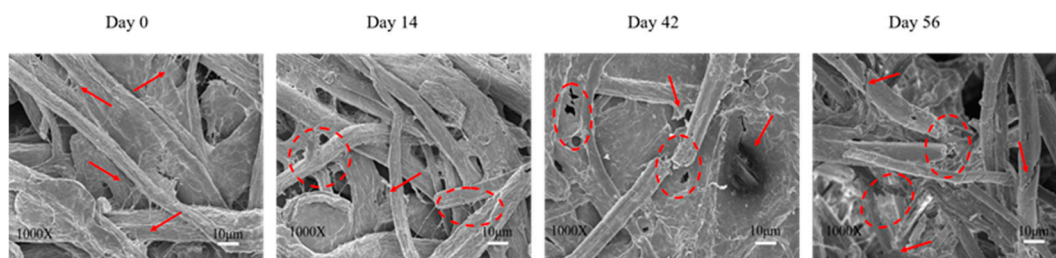
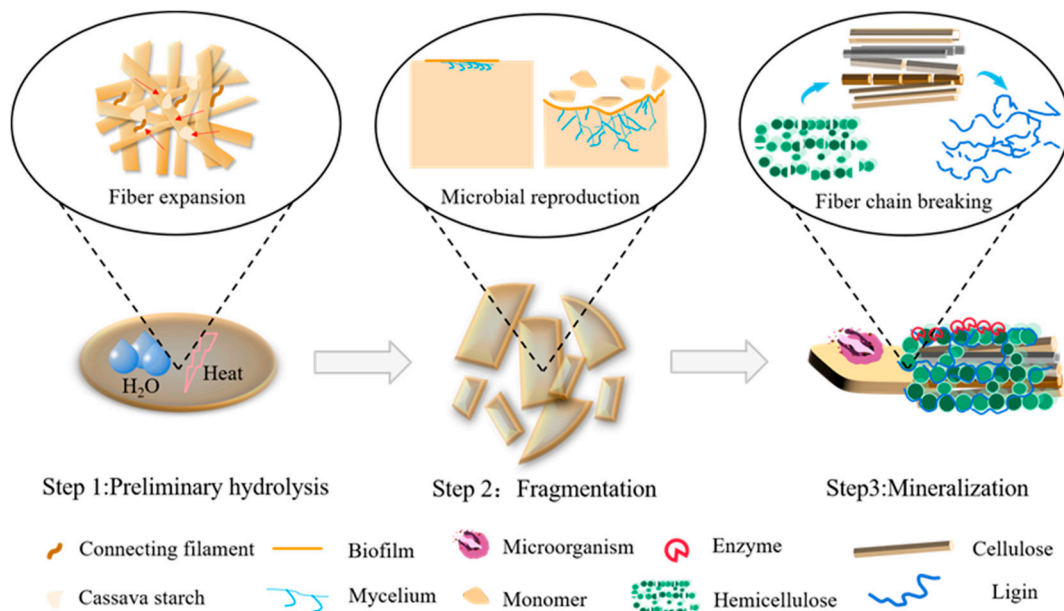


Figure 7. Relative crystallinity of environment-friendly bamboo fiber lunch box in different degradation stages.



(a)



(b)

Figure 8. Microscopic images of environment-friendly bamboo fiber lunch boxes in different degradation stages: (a) microscopic images; (b) microscopic degradation process of the bamboo fiber lunch box.

Figure 8b shows the microscopic degradation process of the lunch box. The lunch box was susceptible to moisture in the initial stage of degradation, as evidenced by the diffusion of large amounts of free water into the pores of the three-dimensional-mesh-interwoven structure composed of bamboo fibers, as well as onto the microfibrils and cassava starch linkage areas. Moisture traveled through the aforementioned capillary structure, where it was bound by hydrogen bonds and van der Waals forces [50,51]. It then continuously absorbed moisture and swelled in amorphous areas such as hemicellulose, resulting in surface hydrolysis [52,53]. Under the action of moisture and heat in the soil, microcracks were generated around the fibers after swelling, which led to structural plasticization and performance degradation.

After long-term exposure to the soil environment, the microorganisms in the soil interacted with the natural fibers mechanically, chemically, or enzymatically [54]. Microbes absorbed starch, polysaccharides, and other nutrients from the bamboo fiber lunch box, and then released mucus substances (mostly polysaccharides and proteins) that stuck to the surface of the lunch box. On the one hand, these mucous substances helped establish a rich biofilm on the surface of the lunch box, enrich the flora, and accelerate the decomposition. On the other hand, they could penetrate the inner interwoven structure of the lunch box together with microorganisms, changing its volume size, pore distribution, and moisture content [55].

Under the combined action of water, heat, and mycelial growth, the lunch box was gradually depolymerized into smaller oligomers and monomer molecules. As microorganisms multiplied, produced enzymes, and extended their mycelia, the number of pores within the bamboo fibers increased. In addition, the fiber matrix expanded, ruptured, and became fragmented. At the same time, the volatilization of small-molecule products also caused an increase in the number of pores. The formed pores accelerated the diffusion of oxygen and enzymes and also debris generation, finally generating CO_2 , H_2O , inorganic salts, and so forth [27].

4. Conclusions

Using an environment-friendly bamboo fiber lunch box made by steam explosion, the degradation performance and mechanism were explored by indoor buried soil degradation. The main conclusions of this study were as follows:

- (1) The environment-friendly bamboo fiber lunch box displayed excellent degradation performance via buried soil degradation. It initially fragmented on day 42 and completely degraded in the soil on day 70. As a product, it had a strength of 44.5 MPa. Durability and easy degradability were combined in the bamboo fiber lunch boxes.
- (2) The degradation mechanism of the soil burial of the lunch box could be roughly divided into three stages: First, the fibers swelled as a result of water and heat in the environment, and the connecting fibrils and tapioca starch dissolved, resulting in a rapid decline in the weight loss rate and mechanical strength. Second, the microorganisms formed rich biofilms, the mycelium expanded, and the substances such as acids and enzymes were secreted to decompose the fibers into oligomers, which were manifested by the decomposition of hemicellulose, cellulose, and other substances and by a gradual decline in the thermal stability. Finally, the residual debris in the soil was gradually decomposed under the action of microorganisms.

Author Contributions: Materials/sampling/trial/data analysis/Writing, H.J.; writing/review/editing, G.W. and F.C.; data analysis, X.C. and X.W.; design/funding support/project administration, G.W. All authors have read and agreed to the published version of the manuscript.

Funding: This research was funded by Beijing Natural Science Foundation (6214039) and the National Natural Science Foundation of China (32171885).

Data Availability Statement: All results from the data analysis needed to evaluate this report are available in the main text or in the tables and figures.

Acknowledgments: Thanks to Chongqing Ruizhu Plant fiber. Co. for materials.

Conflicts of Interest: The authors declare no conflict of interest.

References

1. Zhou, Y.; Shan, Y.; Guan, D.; Liang, X.; Cai, Y.; Liu, J.; Xie, W.; Xue, J.; Ma, Z.; Yang, Z. Sharing tableware reduces waste generation, emissions and water consumption in China's takeaway packaging waste dilemma. *Nat. Food* **2020**, *1*, 552–561. [[CrossRef](#)]
2. Liu, J.; Zhang, T.; Piché-Choquette, S.; Wang, G.; Li, J. Microplastic Pollution in China, an Invisible Threat Exacerbated by Food Delivery Services. *Bull. Environ. Contam. Toxicol.* **2021**, *107*, 778–785. [[CrossRef](#)] [[PubMed](#)]
3. Lebreton, L.; Andrady, A. Future scenarios of global plastic waste generation and disposal. *Palgrave. Commun.* **2019**, *5*, 1–11. [[CrossRef](#)]
4. de Souza Machado, A.A.; Kloas, W.; Zarfl, C.; Hempel, S.; Rillig, M.C. Microplastics as an emerging threat to terrestrial ecosystems. *Glob. Chang. Biol.* **2018**, *24*, 1405–1416. [[CrossRef](#)] [[PubMed](#)]
5. Galloway, T.S.; Cole, M.; Lewis, C. Interactions of microplastic debris throughout the marine ecosystem. *Nat. Ecol. Evol* **2017**, *1*, 1–8. [[CrossRef](#)]
6. Pabortsava, K.; Lampitt, R.S. High concentrations of plastic hidden beneath the surface of the Atlantic Ocean. *Nat. Commun.* **2020**, *11*, 1–11. [[CrossRef](#)]
7. Van Cauwenbergh, L.; Devriese, L.; Galgani, F.; Robbens, J.; Janssen, C.R. Microplastics in sediments: A review of techniques, occurrence and effects. *Mar. Environ. Res.* **2015**, *111*, 5–17. [[CrossRef](#)]
8. Wagner, M.; Scherer, C.; Alvarez-Muñoz, D.; Brennholt, N.; Bourrain, X.; Buchinger, S.; Fries, E.; Grosbois, C.; Klasmeier, J.; Marti, T.; et al. Microplastics in freshwater ecosystems: What we know and what we need to know. *Environ. Sci. Eur.* **2014**, *26*, 1–9. [[CrossRef](#)]
9. Gautam, A.M.; Caetano, N. Study, design and analysis of sustainable alternatives to plastic takeaway cutlery and crockery. *Energy Procedia* **2017**, *136*, 507–512. [[CrossRef](#)]
10. Chen, X.; Wang, G.; Chen, F.; Ye, H.; Jiang, H.; Wang, J. Disposable bamboo fiber dishware: Research state and development prospect. *World Bamboo Ratt.* **2022**, *20*, 6–12.
11. Anna, K. Disposable Food Packaging and Serving Materials—Trends and Biodegradability. *Polymers* **2021**, *13*, 3606.
12. Diao, X.; Wen, Y.; Song, X.; Zhou, Y.; Fu, Y. Current development situation of biodegradable plastic industry in China and abroad. *China Plast.* **2020**, *34*, 123–135.
13. Céline, A.; Fréour, S.; Jacquemin, F.; Casari, P. The hygroscopic behavior of plant fibers: A review. *Front. Chem.* **2014**, *1*, 43. [[CrossRef](#)] [[PubMed](#)]
14. Liu, L.; Lei, Y.; Chen, G. Research on the preparation and properties of water resistant and oil resistant paper tableware made by bagasse brown pulp. *Singapore* **2018**, *477*, 609–615.
15. Pan, P.; Inoue, Y. Polymorphism and isomorphism in biodegradable polyesters. *Prog. Polym. Sci.* **2009**, *34*, 605–640. [[CrossRef](#)]
16. Li, Z.; Rabnawaz, M.; Sarwar, M.G.; Khan, B.; Nair, A.K.; Sirinakbumrung, N.; Kamdem, D.P. A closed-loop and sustainable approach for the fabrication of plastic-free oil-and water-resistant paper products. *Green Chem.* **2019**, *21*, 5691–5700. [[CrossRef](#)]
17. Rosenmai, A.K.; Taxvig, C.; Svingen, T.; Trier, X.; van Vugt-Lussenburg, B.M.A.; Pedersen, M.; Lesné, L.; Jégou, B.; Vinggaard, A.M. Fluorinated alkyl substances and technical mixtures used in food paper-packaging exhibit endocrine-related activity in vitro. *Andrology* **2016**, *4*, 662–672. [[CrossRef](#)]
18. Zaaba, N.F.; Jaafar, M. A review on degradation mechanisms of polylactic acid: Hydrolytic, photodegradative, microbial, and enzymatic degradation. *Polym. Eng. Sci.* **2020**, *60*, 2061–2075. [[CrossRef](#)]
19. Rudnik, E.; Briassoulis, D. Degradation behaviour of poly (lactic acid) films and fibres in soil under Mediterranean field conditions and laboratory simulations testing. *Ind. Crops. Prod.* **2011**, *33*, 648–658. [[CrossRef](#)]
20. Ferreira, D.C.; Molina, G.; Pelissari, F.M. Biodegradable trays based on cassava starch blended with agroindustrial residues. *Composites Part. B* **2020**, *183*, 107682. [[CrossRef](#)]
21. Buxoo, S.; Jeetah, P. Feasibility of producing biodegradable disposable paper cup from pineapple peels, orange peels and Mauritian hemp leaves with beeswax coating. *SN Appl. Sci.* **2020**, *2*, 1–15. [[CrossRef](#)]
22. Wei, X.; Wang, G.; Smith, L.M.; Chen, X.; Jiang, H. Effects of gradient distribution and aggregate structure of fibers on the flexibility and flexural toughness of natural moso bamboo (*Phyllostachys edulis*). *J. Mater. Res. Technol.* **2022**, *16*, 853–863. [[CrossRef](#)]
23. Wei, X.; Wang, G.; Chen, X.; Jiang, H.; Smith, L.M. Natural bamboo coil springs with high cyclic-compression durability fabricated via a hydrothermal-molding-fixing method. *Ind. Crops Prod.* **2022**, *184*, 115055. [[CrossRef](#)]
24. Kim, H.S.; Kim, H.J.; Lee, J.W.; Choi, I.G. Biodegradability of bio-flour filled biodegradable poly (butylene succinate) bio-composites in natural and compost soil. *Polym. Degrad. Stab.* **2006**, *91*, 1117–1127. [[CrossRef](#)]
25. Wei, L.; Liang, S.; McDonald, A.G. Thermophysical properties and biodegradation behavior of green composites made from polyhydroxybutyrate and potato peel waste fermentation residue. *Ind. Crops Prod.* **2015**, *69*, 91–103. [[CrossRef](#)]
26. Chan, C.M.; Vandi, L.J.; Pratt, S.; Halley, P.; Richardson, D.; Werker, A.; Laycock, B. Insights into the biodegradation of PHA/wood composites: Micro-and macroscopic changes. *Sustainable. Mater. Technol.* **2019**, *21*, e00099. [[CrossRef](#)]
27. Zambrano, M.C.; Pawlak, J.J.; Venditti, R.A. Effects of chemical and morphological structure on biodegradability of fibers, fabrics, and other polymeric materials. *BioResources* **2020**, *15*, 9786. [[CrossRef](#)]

28. National Standards of P. R. China, Evaluation of the potential biodegradation and disintegration ability of materials under the action of specific microorganisms. GB/T 19275–2003. Available online: <https://max.book118.com/html/2018/0427/163421514.shtm> (accessed on 2 February 2004).
29. National Standards of P. R. China, Plastic-Determination of tensile properties-Part 3: Test conditions for films and sheets. GB/T 1040.3–2006. Available online: <https://max.book118.com/html/2020/0601/8061045061002114.shtm> (accessed on 1 February 2007).
30. Ibrahim, H.; Mehanny, S.; Darwish, L.; Farag, M. A comparative study on the mechanical and biodegradation characteristics of starch-based composites reinforced with different lignocellulosic fibers. *J. Polym. Environ.* **2018**, *26*, 2434–2447. [[CrossRef](#)]
31. Van Soest, P.J.; Robertson, J.B.; Lewis, B.A. Methods for dietary fiber, neutral detergent fiber, and non-starch polysaccharides in relation to animal nutrition. *J. Dairy Sci.* **1991**, *74*, 3583–3597. [[CrossRef](#)]
32. Lionetto, F.; Del Sole, R.; Cannoletta, D.; Vasapollo, G.; Maffezzoli, A. Monitoring wood degradation during weathering by cellulose crystallinity. *Materials* **2012**, *5*, 1910–1922. [[CrossRef](#)]
33. Li, X.; Zhang, M. Study on the relationship between wood moisture content and crystallinity by X-ray diffraction. *J. Northeast. For. Univ.* **2014**, *42*, 97–99.
34. Yang, F.; Long, H.; Xie, B.; Zhou, W.; Luo, Y.; Zhang, C.; Dong, X. Mechanical and biodegradation properties of bamboo fiber-reinforced starch/polypropylene biodegradable composites. *J. Appl. Polym. Sci.* **2020**, *137*, 48694. [[CrossRef](#)]
35. Liu, C.; Luan, P.; Li, Q.; Cheng, Z.; Sun, X.; Cao, D.; Zhu, H. Biodegradable, hygienic, and compostable tableware from hybrid sugarcane and bamboo fibers as plastic alternative. *Matter* **2020**, *3*, 2066–2079. [[CrossRef](#)]
36. Badji, C.; Beigbeder, J.; Garay, H.; Bergeret, A.; Benezet, J.C.; Desauziers, V. Exterior and under glass natural weathering of hemp fibers reinforced polypropylene biocomposites: Impact on mechanical, chemical, microstructural and visual aspect properties. *Polym. Degrad. Stab.* **2018**, *148*, 104–116. [[CrossRef](#)]
37. Badji, C.; Socalingame, L.; Garay, H.; Bergeret, A.; Bénézet, J.C. Influence of weathering on visual and surface aspect of wood plastic composites: Correlation approach with mechanical properties and microstructure. *Polym. Degrad. Stab.* **2017**, *137*, 162–172. [[CrossRef](#)]
38. Phetwarotai, W.; Potiyaraj, P.; Aht-Ong, D. Biodegradation of polylactide and gelatinized starch blend films under controlled soil burial conditions. *J. Polym. Environ.* **2013**, *21*, 95–107. [[CrossRef](#)]
39. Wool, R.P.; Raghavan, D.; Wagner, G.C.; Billieux, S. Biodegradation dynamics of polymer–starch composites. *J. Appl. Polym. Sci.* **2000**, *77*, 1643–1657. [[CrossRef](#)]
40. Kalka, S.; Huber, T.; Steinberg, J.; Baronian, K.; Müssig, J.; Staiger, M.P. Biodegradability of all-cellulose composite laminates. *Composites Part. A* **2014**, *59*, 37–44. [[CrossRef](#)]
41. Zakikhani, P.; Zahari, R.; Sultan, M.T.H.; Majid, D.L.A.A. Thermal degradation of four bamboo species. *BioResources* **2016**, *11*, 414–425. [[CrossRef](#)]
42. Asim, M.; Jawaid, M.; Nasir, M.; Saba, N. Effect of fiber loadings and treatment on dynamic mechanical, thermal and flammability properties of pineapple leaf fiber and kenaf phenolic composites. *J. Renewable Mater.* **2018**, *6*, 383–393. [[CrossRef](#)]
43. Asim, M.; Paridah, M.T.; Chandrasekar, M.; Shahroze, R.M.; Jawaid, M.; Nasir, M.; Siakeng, R. Thermal stability of natural fibers and their polymer composites. *Iran. Polym. J.* **2020**, *29*, 625–648. [[CrossRef](#)]
44. Yang, W.; Fortunati, E.; Dominici, F.; Kenny, J.M.; Puglia, D. Effect of processing conditions and lignin content on thermal, mechanical and degradative behavior of lignin nanoparticles/poly(lactic acid) bionanocomposites prepared by melt extrusion and solvent casting. *Eur. Polym. J.* **2015**, *71*, 126–139. [[CrossRef](#)]
45. Dorez, G.; Taguet, A.; Ferry, L.; Lopez-Cuesta, J.M. Thermal and fire behavior of natural fibers/PBS biocomposites. *Polym. Degrad. Stab.* **2013**, *98*, 87–95. [[CrossRef](#)]
46. Li, X.; Sun, C.; Zhou, B.; He, Y. Determination of Hemicellulose, Cellulose and Lignin in Moso Bamboo by Near Infrared Spectroscopy. *Sci. Rep.* **2015**, *5*, 17210. [[CrossRef](#)] [[PubMed](#)]
47. Singh, R.; Upadhyay, S.K.; Rani, A.; Kumar, P.; Kumar, A.; Singh, C. Lignin biodegradation in nature and significance. *Vegetos* **2018**, *31*, 39–44. [[CrossRef](#)]
48. Cho, C.H.; Lee, K.H.; Kim, J.S.; Kim, Y.S. Micromorphological characteristics of bamboo (*Phyllostachys pubescens*) fibers degraded by a brown rot fungus (*Gloeophyllum trabeum*). *J. Wood Sci.* **2008**, *54*, 261–265. [[CrossRef](#)]
49. Faix, O. Classification of Lignins from Different Botanical Origins by FT-IR Spectroscopy. *Holzforschung* **1991**, *45*, 21–28. [[CrossRef](#)]
50. Wei, X.; Yuan, J.; Wang, G.; Chen, F.; Chen, X.; Jiang, H.; Smith, L.M.; Deng, J. Effect of chemical composition and cell structure on water vapor sorption behavior of parenchyma cells and fiber cells in moso bamboo (*Phyllostachys edulis*). *Ind. Crops Prod.* **2022**, *178*, 114652. [[CrossRef](#)]
51. Wohler, M.; Bensefelt, T.; Wågberg, L.; Furó, I.; Berglund, L.A.; Wohler, J. Cellulose and the role of hydrogen bonds: Not in charge of everything. *Cellulose* **2021**, 1–23. [[CrossRef](#)]
52. Kabir, E.; Kaur, R.; Lee, J.; Kim, K.H.; Kwon, E.E. Prospects of biopolymer technology as an alternative option for non-degradable plastics and sustainable management of plastic wastes. *J. Cleaner Prod.* **2020**, *258*, 120536. [[CrossRef](#)]
53. Azwa, Z.N.; Yousif, B.F.; Manalo, A.C.; Karunasena, W. A review on the degradability of polymeric composites based on natural fibres. *Mater. Des.* **2013**, *47*, 424–442. [[CrossRef](#)]

-
54. Gu, J.D. Microbiological deterioration and degradation of synthetic polymeric materials: Recent research advances. *Int. Biodeterior. Biodegrad.* **2003**, *52*, 69–91. [[CrossRef](#)]
 55. Lucas, N.; Bienaime, C.; Belloy, C.; Queneudec, M.; Silvestre, F.; Nava-Saucedo, J.E. Polymer biodegradation: Mechanisms and estimation techniques. *Chemosphere* **2008**, *73*, 429–442. [[CrossRef](#)] [[PubMed](#)]